RSC Advances

PAPER

View Article Online
View Journal | View Issue

Cite this: *RSC Adv.*, 2017, **7**, 37699

pH-Responsive wormlike micelles based on microstructural transition in a C_{22}-tailed cationic surfactant–aromatic dibasic acid system

Pengxiang Wang, Wanli Kang,* Hongbin Yang,* Xia Yin, Yilu Zhao, Zhou Zhu and Xiangfeng Zhang

Received 23rd June 2017
Accepted 23rd July 2017

DOI: 10.1039/c7ra07000d

rsc.li/rsc-advances

pH-Responsive wormlike micelles based on microstructural transition, and formed by complexation of *N*-erucamidopropyl-*N*,*N*-dimethylamine (UC_{22}AMPM) and potassium phthalic acid (PPA) at a molar ratio of 2 : 1, were developed and compared with CTAB/PPA at the same molar ratio. Phase behavior, viscoelasticity, and microstructural transitions of solutions were investigated by observing their appearance, rheological characteristics, dynamic light scattering, and ^{1}H NMR measurements. It was found that the phase behavior of UC_{22}AMPM/PPA solutions undergoes transitions from transparent viscoelastic fluid to phase separation with white floaters upon increasing pH. By increasing pH from 2.01 to 6.19, the viscosity of wormlike micelles in the transparent solutions continuously increased and reached ~1.4 × 10^6 mPa s at pH 6.19. As pH was adjusted to 7.32, the opalescent solution showed a water-like flowing behaviour and the η_0 rapidly declined to ~1.7 mPa s. The viscosity of the CTAB/PPA solutions had a maximum at pH 2.98 and then decreased with increasing pH. This radical variation in rheological behavior is attributed to the pH dependent hydrophobicity of PPA and ultra-long hydrophobic chain of UC_{22}AMPM. Additionally, dramatic viscosity changes of about 6 magnitudes can be triggered by varying pH without any deterioration for the UC_{22}AMPM/PPA system.

Introduction

Wormlike micelles (WLMs) have attracted growing interest due to their unique properties in the past few years.[1–9] These types of micelles, with contour lengths ranging from several nanometres up to several micrometres, are usually self-assembled from aqueous surfactant solutions. They may overlap and entangle to form three-dimensional network structures which exhibit viscoelastic properties. Hitherto, the fascinating properties of WLMs render them extremely useful in many aspects of industrial applications including oil production,[10–12] drag reduction agents,[13,14] and drug delivery.[15–17]

Recently, particular interest has been focused on the design of WLMs that are responsive to external stimuli, such as pH,[18–23] CO_2,[24–26] light,[27–29] and temperature.[30–34] These stimuli-responsive viscoelastic fluids produced by WLMs can find applications in transmission clutches,[35] shock absorbers,[36] vibration control,[37] human muscle stimulators, and clean fracturing fluids.[11,38] Compared to other external stimuli, pH is a simple and economical trigger for controlling viscoelasticity of WLMs solutions. To date, pH-responsive WLMs have been mainly formed by mixing a cationic surfactant and a low molecular weight hydrotrope that screen electrostatic repulsions between the surfactant charged headgroups. Among these hydrotropes, phthalic acid has been widely used. For example, Lin *et al.*[39] introduced potassium phthalic acid (PPA) as a pH-responsive hydrotrope into the cationic surfactant cetyltrimethylammonium bromide (CTAB) solution to design pH-responsive WLMs. This viscoelastic fluid can be switched between a highly viscoelastic solution and a water-like solution within a narrow pH range, which was attributed to a transition from WLMs to short cylindrical micelles. More recently, Rose *et al.*[40] proposed pH-dependent changes in the micellar binding ability of phthalic acid as the key factor regulating reversible switching between liquid-like and gel-like states on adjusting the pH of cetylpyridinium chloride (CPC)/phthalic acid solutions. However, the viscosity of these systems decreased rapidly with an increase of pH when the pH was more than 3.00. And none of these experiments focused on understanding the microstructural changes and underlying molecular interactions that brought about the pH-responsive rheological behavior (Scheme 1).

Scheme 1 The chemical structure of *N*-erucamidopropyl-*N*,*N*-dimethylamine (UC_{22}AMPM).

School of Petroleum Engineering, China University of Petroleum (East China), Qingdao 266580, Shandong, P. R. China. E-mail: kangwanli@126.com; yhb0810@126.com

Since these surfactants, which are bearing hydrophobic chains shorter than C_{18}, cannot form wormlike micelles spontaneously by themselves, the addition of organic or inorganic hydrotropes is inevitably necessary.[41–43] To address this, several kinds of surfactants that bear a C_{22}-tail have been investigated.[44–46] Protonated *N*-erucamidopropyl-*N*,*N*-dimethylamine (UC_{22}AMPM) is a cationic surfactant which can form the WLMs without any hydrotropes when pH is less than 6.20, and the addition of an inorganic polyacid improved the formation of "oligomeric" surfactants which significantly increased viscoelasticity of the system.[5,47] But the combination of UC_{22}AMPM and PPA has not been reported so far, and we believed this ultra-long hydrophobic chain will have an unusual impact on the performance of the mixed system.

Consequently, we investigated pH-responsive structural changes in aqueous UC_{22}AMPM/PPA solutions through a combination of observing their appearance, rheology, dynamic light scattering (DLS), and ^{1}H NMR measurements. Our results show an unexpected rheological behavior with changing pH and offer new insights into microstructural evolution controlling self-assembly in cationic surfactant–aromatic dibasic acid mixtures.

Experimental

Materials

UC_{22}AMPM with purity greater than 99.0% (HPLC) was synthesized based on a procedure previously reported.[47] Cetyltrimethylammonium bromide (CTAB), potassium phthalic acid (PPA), hydrochloric acid (HCl) and sodium hydroxide (NaOH) were all analytical grades and purchased from Beijing Chemical Company (China). Water used was triply distilled by a quartz water purification system. All reagents were used without further treatment.

Sample preparation

Samples were obtained by mixing 30 mM UC_{22}AMPM with 15 mM PPA in distilled water; then it was well-mixed and followed by magnetic agitation for several minutes. The pH values of the UC_{22}AMPM/PPA system were regulated by adding HCl and/or NaOH aqueous solutions dropwise. Generally, for freshly prepared wormlike micellar solutions, the samples were left at room temperature for at least 1 day prior to measurements. The CTAB/PPA system was prepared in the same manner as described above.

Rheology

Rheological experiments were performed on a Physica MCR 301 (Anton Paar, Austria) rotational rheometer equipped with a searle-type concentric cylinder geometry CC27 (ISO3219). Samples were equilibrated at the temperature of interest for no less than 20 min prior to measurements. Dynamic frequency spectra were conducted in the linear viscoelastic regime of the samples, as determined from dynamic stress sweep measurements. The temperature was set to +0.1 °C accuracy using a Peltier temperature control device.

Dynamic light scattering (DLS)

DLS was performed with a spectrometer (ALV-5000/E/WIN Multiple Tau Digital Correlator) and a Spectra-Physics 2017 200 mW Ar laser (514.5 nm wavelength). The scattering angle was 90°, and the intensity autocorrelation functions were analyzed by using the methods of Contin.

^{1}H NMR

^{1}H NMR was carried out in solutions of D_2O with Mercury Plus 300 MHz. The NMR measurement was carried out at 25 °C.

Results and discussion

Comparison of zero-shear viscosity variations induced by pH

The effect of pH on zero-shear viscosity (η_0) variation of the UC_{22}AMPM/PPA system is shown in Fig. 1. The η_0 is $\sim 2.8 \times 10^4$ mPa s at pH 2.01 for 30 mM UC_{22}AMPM/15 mM PPA solution. When the pH was increased to 6.19, the η_0 reached to $\sim 1.4 \times 10^6$ mPa s, which was improved about 50 times and nearly enough to support its own weight. When further increasing the pH, the η_0 rapidly declined to $\sim$1.7 mPa s and this character remained almost unchanged up to pH 9.17. As a comparison, the η_0 of 30 mM CTAB/15 mM PPA was also investigated. It is noteworthy that this solution showed a volcano change when pH was increased from 2.01 to 6.19, while the viscosity of the UC_{22}AMPM/PPA system increased monotonously in that same pH range. Furthermore, the η_0 of CTAB/PPA is smaller than that of the UC_{22}AMPM/PPA solution at the same pH; the reason may be due to different structures of the two surfactants. Compared with CTAB, UC_{22}AMPM has an ultra-long hydrophobic carbon chain. Thus, an increase in the aggregate parameter p can be expected,[48,49] and the formation of larger aggregates with low curvature is more favored. The variation of η_0 also reflects that pH has a significantly different effect on these two systems, since the chemical structures of two surfactants are without any variation within the pH range from 2.01 to 6.19. Therefore, we

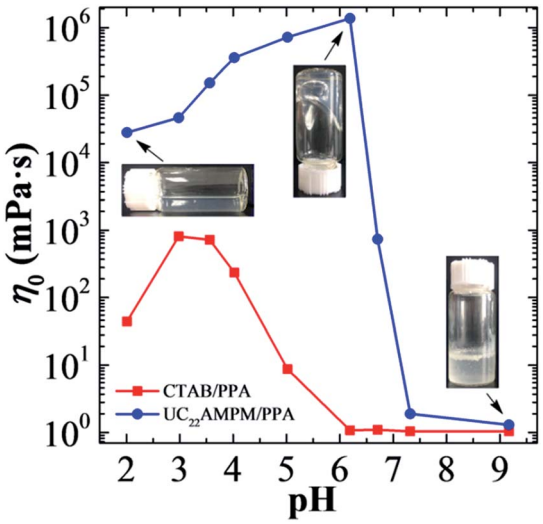

Fig. 1 The appearance and zero-shear viscosity variations induced by pH.

speculate that the radical variations in rheological behavior between the two systems were caused by the pH-sensitivity of PPA.

pH-Responsive viscoelastic behavior in UC_{22}AMPM/PPA system

As mentioned above, pH has an extra significant effect on the η_0 of the UC_{22}AMPM/PPA system, so the rheological properties of this system under different pH conditions were further studied. As shown in Fig. 2a, when the pH ranged from 2.01–6.71, it can be seen that all solutions show shear-thinning behavior when the shear rate exceeds a critical shear rate, indicating the presence of WLMs in all solutions. When the pH is higher than 7.32, the apparent viscosity of the solution remains constant regardless of the shear rate, which is typical of Newtonian fluid. It is known that viscosity is related to the type and morphology of various aggregates, and the viscosity variation of the UC_{22}-AMPM/PPA solution has an abrupt massive change which reflects growth first and then sharp decrease of the wormlike micelles. The plots of the elastic (G') and viscous modulus (G'') are shown as a function of oscillatory shear frequency (ω) for UC_{22}AMPM/PPA solutions at different pH in Fig. 2b. All solutions exhibit a typical viscoelastic response and the viscoelasticity of them is attributed to entanglement of long WLMs to form a transient network. It is easy to see that the viscoelastic behavior of these solutions are like a strongly elastic gel where the values of G' are always higher than G'' when the pH ranged from 2.01 to 6.19. The relaxation time τ_R can be determined from the reciprocal of the frequency at the crossover of G' and G'', which is proportional to the average micelle length. However, the ω_c values of UC_{22}AMPM/PPA solutions are too low to detect, so the relaxation time τ_R is extremely long.

Results of microstructure variations at different pH values can be derived from the macroscopical pH-responsive rheological behaviors of the UC_{22}AMPM/PPA aqueous system. To further confirm micelle transition from a micro perspective, DLS measurements were carried out to investigate the microscopic structures at four different pH values. As demonstrated in Fig. 3, the average hydrodynamic radius of 13.5 nm gained at initial pH 2.01. When pH increased to 4.02, two peaks in the plot appeared with average hydrodynamic diameters of 21.0 nm and 4800.7 nm, respectively. This phenomenon indicates that different growth degrees of micelles are coexistent at that pH. Then, the two peaks continued moving right and the intensity of 50.7 nm decreased with an increase at 5559.6 nm when pH arrived at 6.19, demonstrating that the micelles gain sufficient growth. However, the peaks move back left and the intensity of higher average hydrodynamic radius almost disappeared with a continued increasing of the pH to 6.71, which can be ascribed to deprotonating of the tertiary amine and more neutral UC_{22}-AMPM occurring in the system. It is also shows the average diameter size as a function of pH (Fig. 3 insert). The average diameter size of aggregates in the UC_{22}AMPM/PPA aqueous system rose with pH to reach a maximum value and then

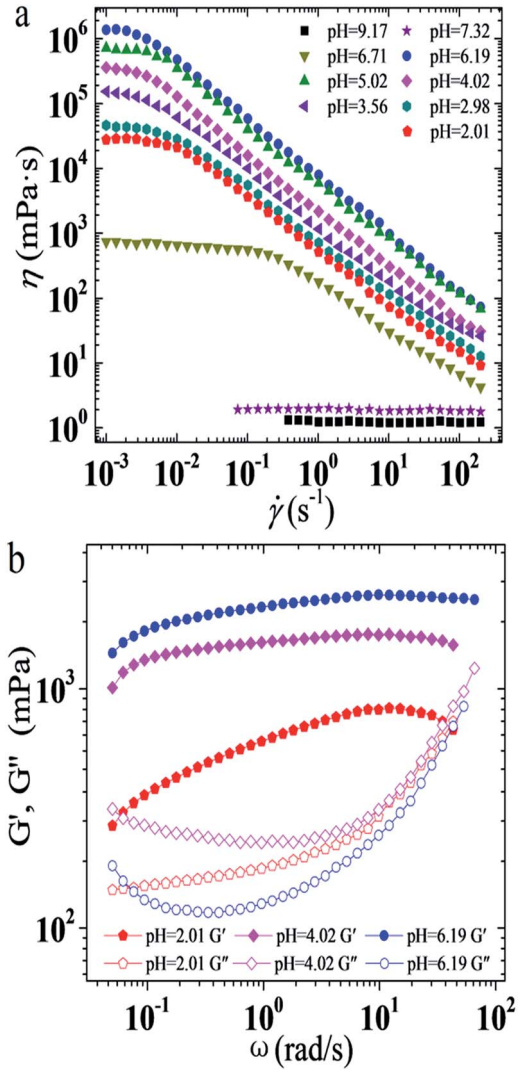

Fig. 2 Effect of pH on steady (a) and dynamic (b) rheological curves for the 30 mM UC_{22}AMPM/15 mM PPA solutions at 25 °C.

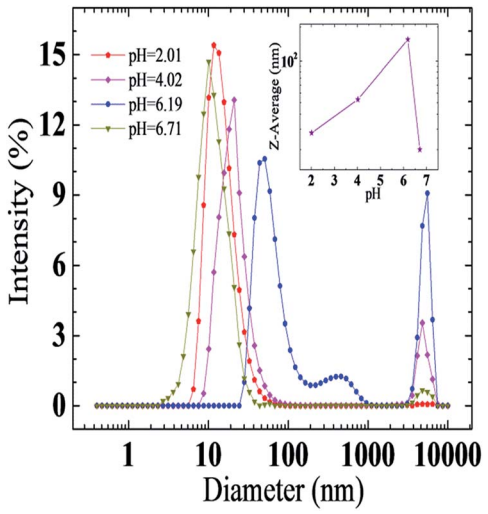

Fig. 3 Effects of pH on the average hydrodynamic diameter of the aggregates at 25 °C. Inset: the average diameter size as a function of pH.

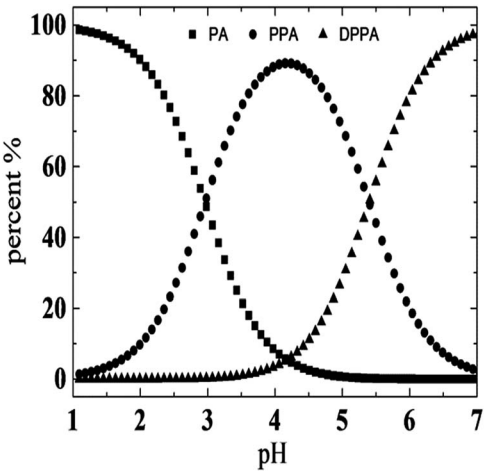

Fig. 4 Species distribution resulting from an aqueous solution of PPA at 25 °C.

declined, implying that the aggregates undergo growth and destruction procedures with increasing pH. The rheological performance of the system was consistent with the test results.

Microstructural transition induced by pH

As mentioned above, we speculate that the structural changes in PPA lead to differences between these two systems. As the pH increased with addition of NaOH, PPA molecules were gradually transformed into DPPA. Fig. 4 shows species distribution of PPA solutions varying with pH values. It is illustrated that PPA and DPPA are the main existence forms for UC_{22}AMPM/PPA and CTAB/PPA solutions when pH values are around 2.96, and higher than 5.40, respectively. In pH ranges from 4.15 to 6.19, the content of PPA gradually decreased with an increase of DPPA.

The solubility of DPPA (~1.5 M) is larger than that of PPA (~0.7 M) due to the special molecular structure of two ionized carboxylic acid moieties.[39] Thus, it can be suggested that DPPA is more hydrophilic than PPA and cannot effectively insert between the surfactant tails acting like hydrotropes to moderately increase the volume of the lipophilic chain. As a result, a loose packing between hydrocarbon chains was adapted in the CTAB/PPA system, and short cylindrical micelles were formed when pH was larger than 3.56. However, UC_{22}AMPM can form wormlike micelles spontaneously on its own. While DPPA cannot insert between the surfactants, the headgroups can promote further closing with each other due to electrostatic attraction and elimination of steric hindrance of the benzene ring. This intermolecular interaction makes DPPA and UC_{22}-AMPM behaved as "pseudo" Gemini surfactants, and a tight packing between hydrocarbon chains was adapted in the UC_{22}AMPM/PPA system. Consequently, this leads to the growth of larger WLMs and the enhancement of corresponding viscosities. Further increasing the pH to larger than 6.19 drops the viscosity rapidly due to deprotonation of the tertiary amine and disintegration of the WLMs. In summary, molecular structure and hydrophobicity of PPA was influenced by pH, which may result in a variation of molecular interactions between surfactants and hydrotropes. As a result, two different pH-responsive macroscopic rheological properties can be obtained by surfactants with different tails. A representative scheme is illustrated in Fig. 5.

NMR spectroscopy is a powerful tool for investigating the association between a hydrotrope and amphiphile in aqueous solutions from the viewpoint of chemical shifts.[50–52] The ^{1}H NMR spectra of 15 mM PPA in the presence and absence of 30 mM UC_{22}AMPM at different pH values are shown in Fig. 6. With the addition of UC_{22}AMPM, different degrees of peak shift are observed at pH 6.19, 5.02, 4.02, and 3.56.

It can be noted that the protons on an aromatic ring show an apparent shift with addition of UC_{22}AMPM: the proton H_1 shifted upfield while the proton H_2 shifted downfield. A similar

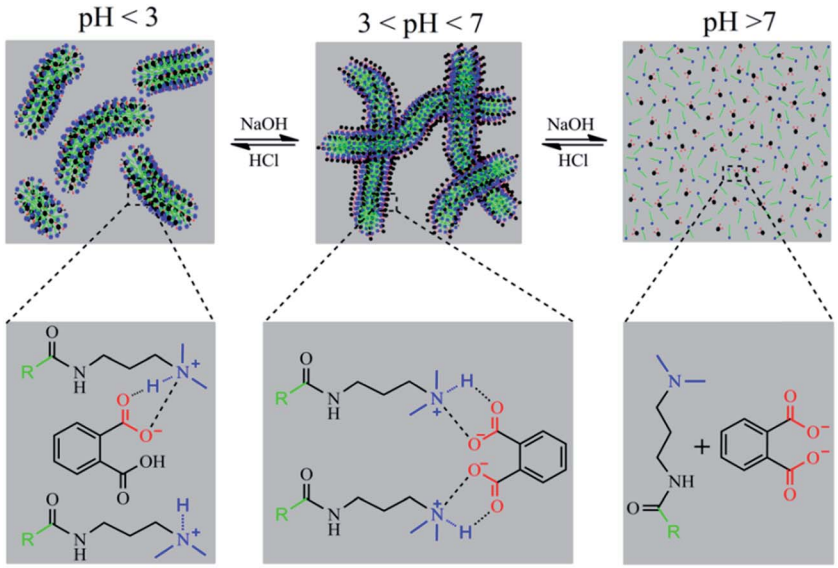

Fig. 5 Schematic representation of microstructures transition mechanism induced by pH in the UC_{22}AMPM/PPA system.

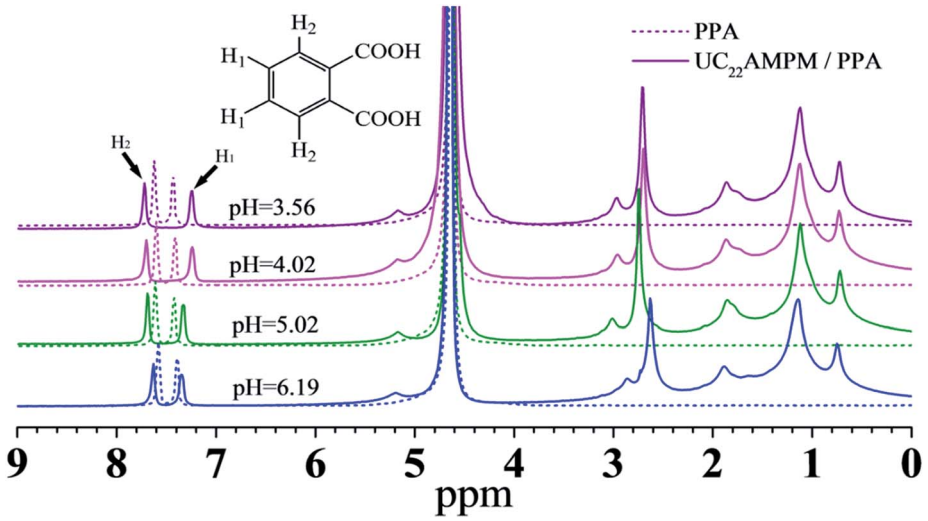

Fig. 6 Proton resonances for 30 mM UC_{22}AMPM/15 mM PPA solution at different pH values.

result was also found in CTAB/PPA aqueous solutions.[39] H_1 was exposed to bulk water and experienced a polar environment in the absence of UC_{22}AMPM; however, with addition of UC_{22}-AMPM, proton H_1 undergoes from a polar environment to a nonpolar environment and as a result the NMR signal shifted upfield. The parameter $\Delta\delta$ was applied to better discuss the effect of pH interaction between UC_{22}AMPM and PPA, which was proposed by Huang and defined as[39]

$$\Delta\delta = \delta' - \delta$$

where δ' and δ are the chemical shifts of the proton on the PPA aromatic rings in the absence and presence of UC_{22}AMPM, respectively. As discussed above, the signal shift change $\Delta\delta$ was caused by changes in the chemical environment. In turn, the value of $\Delta\delta$ can scale the environment of PPA qualitatively.

A plot of $\Delta\delta$ (H_1) and $\Delta\delta$ (H_2) as a function of pH value is shown in Fig. 7. Note that the signal shift change $\Delta\delta$ for both H_1 and H_2 is gradually reduced as the pH rises. Considering that $\Delta\delta$ was caused by changes in chemical environment, decrease of $\Delta\delta$ (H_1) and $\Delta\delta$ (H_2) means that the environment of aggregates transfers from a nonpolar environment to polar environment, and confirms that DPPA entered the aqueous phase from a micelle with an increase of pH.

Cryo-TEM images of UC_{22}AMPM/PPA solutions are shown in Fig. 8. When the pH is 2.01, there are high-density wormlike micelles with relatively shorter lengths in the solution and the flexible worms can also entangle with each other to form aggregates of networks. When the pH increases to 6.19 (Fig. 8b), the length of micelles can reach to hundreds of nanometres or even several micrometres. The micelles are also found to overlap with each other and entangle to form three-dimensional network structures.

The above results reflect the remarkable effects of pH on the viscoelastic behaviors of a UC_{22}AMPM/PPA solution. As we can see, the rheological properties of the solution can also be reversibly switched *via* a facile way of tuning pH through the addition of acid or base in small amounts (Fig. 9). The viscosity of a solution changes between $\sim 1.4 \times 10^6$ and ~ 1.7 mPa s and, at the same time, the flow state of the solution turns between gel-like and water-like states for at least three cycles without any deterioration. This high pH sensitivity and reversible control of rheological properties may greatly facilitate practical applications of such a responsive viscoelastic fluid.

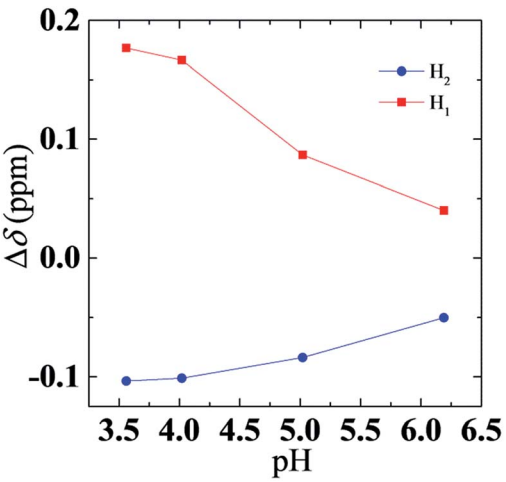

Fig. 7 Variation of proton chemical shift change $\Delta\delta$ on the aromatic ring at different pH.

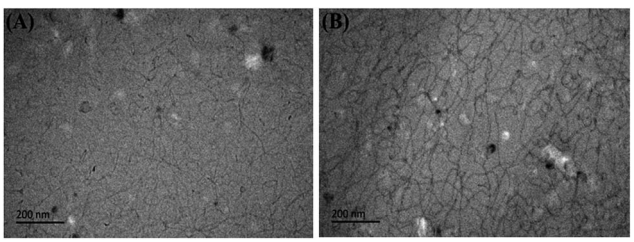

Fig. 8 Cryo-TEM images for 30 mM UC_{22}AMPM/15 mM PPA at pH 2.01 (A) and 6.19 (B).

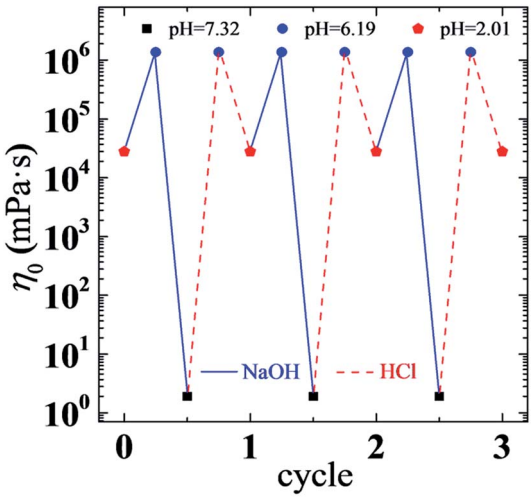

Fig. 9 pH-Switchable viscosity of 30 mM UC_{22}AMPM/15 mM PPA solution at 25 °C.

Conclusions

A pH-responsive wormlike micelle based on a "pseudo" Gemini surfactant was developed by complexation of UC_{22}AMPM and PPA with a molar ratio of 2 : 1 and compared with a CTAB/PPA system. The UC_{22}AMPM/PPA system has a wider range of pH-responsiveness and a different variation of viscosity; the appearance of aqueous states with a pH range of 2.01 to 9.17 depends on hydrophobicity of PPA and ionization of UC_{22}-AMPM. Rheological results and ^{1}H NMR spectroscopy correspondingly revealed the microstructure's transition. The viscosity of the UC_{22}AMPM/PPA system is much higher and adjustable because of the variation from monomer to a "Gemini" surfactant. The WLMs system also has excellent pH reversible ability for at least 3 circles of pH regulation, which is very important for its practical applications.

Acknowledgements

The work was supported by the Fundamental Research Funds for the Central Universities (16CX06032A, 15CX08003A), the National Natural Science Foundation of China (21273286), the China Postdoctoral Science Foundation (2017M612378), Scientific Research Fund for Introducing Scholars of China University of Petroleum (YJ201601088) and Qingdao Postdoctoral Application Research Project (2016222).

References

1 Z. Chu, C. A. Dreiss and Y. Feng, *Chem. Soc. Rev.*, 2013, **42**, 7174–7203.
2 A. Wang, W. Shi, J. Huang and Y. Yan, *Soft Matter*, 2016, **12**, 337–357.
3 T. Kusano, K. Akutsu, H. Iwase, T. Yoshimura and M. Shibayama, *Colloids Surf., A*, 2016, **497**, 109–116.
4 C. Dai, W. Li, Y. Cui, Y. Sun, W. Wu, Z. Xu, Y. Liu, Z. Yang and X. Wu, *Colloids Surf., A*, 2016, **500**, 32–39.
5 Y. Feng and Z. Chu, *Soft Matter*, 2015, **11**, 4614–4620.
6 S. A. Rogers, M. A. Calabrese and N. J. Wagner, *Curr. Opin. Colloid Interface Sci.*, 2014, **19**, 530–535.
7 T. Kusano, H. Iwase, T. Yoshimura and M. Shibayama, *Langmuir*, 2012, **28**, 16798–16806.
8 Y. Hou, Y. Han, M. Deng, J. Xiang and Y. Wang, *Langmuir*, 2010, **26**, 28–33.
9 Y. Feng, Z. Chu and C. A. Dreiss, in *Smart Wormlike Micelles: Design, Characteristics and Applications*, Springer Berlin Heidelberg, Berlin, Heidelberg, 2015.
10 C. Dai, K. Wang, Y. Liu, J. Fang and M. Zhao, *PLoS One*, 2014, **9**, e113723.
11 E. S. Boek, A. Jusufi, H. Löwen and G. C. Maitland, *J. Phys.: Condens. Matter*, 2002, **14**, 9413.
12 M. S. Kamal, *J. Surfactants Deterg.*, 2016, **19**, 223–236.
13 H. Shi, W. Ge, Y. Wang, B. Fang, J. T. Huggins, T. A. Russell, Y. Talmon, D. J. Hart and J. L. Zakin, *J. Colloid Interface Sci.*, 2014, **418**, 95–102.
14 H. Shi, W. Ge, H. Oh, S. M. Pattison, J. T. Huggins, Y. Talmon, D. J. Hart, S. R. Raghavan and J. L. Zakin, *Langmuir*, 2013, **29**, 102–109.
15 N. Hassan, J. M. Ruso and A. González-Pérez, *Soft Matter*, 2011, **7**, 5194.
16 D. P. Acharya and H. Kunieda, *J. Phys. Chem. B*, 2003, **107**, 10168–10175.
17 H. Afifi, G. Karlsson, R. K. Heenan and C. A. Dreiss, *Langmuir*, 2011, **27**, 7480–7492.
18 H. Lu, Q. Shi and Z. Huang, *J. Phys. Chem. B*, 2014, **118**, 12511–12517.
19 Y. Lin, X. Han, X. Cheng, J. Huang, D. Liang and C. Yu, *Langmuir*, 2008, **24**, 13918–13924.
20 Z. Yan, C. Dai, M. Zhao, G. Zhao, Y. Li, X. Wu, M. Du and Y. Liu, *Colloids Surf., A*, 2015, **482**, 283–289.
21 Z. Chu and Y. Feng, *Chem. Commun.*, 2010, **46**, 9028–9030.
22 L. Zhao, K. Wang, L. Xu, Y. Liu, S. Zhang, Z. Li, Y. Yan and J. Huang, *Soft Matter*, 2012, **8**, 9079–9085.
23 C. B. Minkenberg, B. Homan, J. Boekhoven, B. Norder, G. J. Koper, R. Eelkema and J. H. van Esch, *Langmuir*, 2012, **28**, 13570–13576.
24 Y. Zhang, Y. Zhang, C. Wang, X. Liu, Y. Fang and Y. Feng, *Green Chem.*, 2016, **18**, 392–396.
25 H. Liu, Y. Zhao, C. A. Dreiss and Y. Feng, *Soft Matter*, 2014, **10**, 6387–6391.
26 Y. Zhang, Y. Feng, J. Wang, S. He, Z. Guo, Z. Chu and C. A. Dreiss, *Chem. Commun.*, 2013, **49**, 4902–4904.
27 K. Jia, J. Hu, J. Dong and X. Li, *J. Colloid Interface Sci.*, 2016, **477**, 156–165.
28 P. Xing, H. Chen, L. Bai and Y. Zhao, *Chem. Commun.*, 2015, **51**, 9309–9312.
29 H. Yan, Y. Long, K. Song, C. H. Tung and L. Zheng, *Soft Matter*, 2014, **10**, 115–121.
30 L. Zhang, W. Kang, D. Xu, J. Jiang, H. Feng, M. Yang, Q. Zhou and H. Wu, *Colloids Surf., A*, 2017, **522**, 628–634.
31 X. L. Wei, C. H. Han, P. P. Geng, X. X. Chen, Y. Guo, J. Liu, D. Z. Sun, J. H. Zhang and M. J. Yu, *Soft Matter*, 2016, **12**, 1558–1566.
32 X. Ji, M. Tian and Y. Wang, *Langmuir*, 2016, **32**, 972–981.

33 C. Morita, Y. Imura, T. Ogawa, H. Kurata and T. Kawai, *Langmuir*, 2013, **29**, 5450–5456.
34 T. S. Davies, A. M. Ketner and S. R. Raghavan, *J. Am. Chem. Soc.*, 2006, **128**, 6669–6675.
35 D. L. Hartsock, R. F. Novak and G. J. Chaundy, *J. Rheol.*, 1991, **35**, 1305–1326.
36 A. M. Ketner, R. Kumar, T. S. Davies, P. W. Elder and S. R. Raghavan, *J. Am. Chem. Soc.*, 2007, **129**, 1553–1559.
37 R. Stanway, J. L. Sproston and A. K. El-Wahed, *Smart Mater. Struct.*, 1996, **5**, 464.
38 K. Bohon and S. Krause, *J. Polym. Sci., Part B: Polym. Phys.*, 1998, **36**, 1091–1094.
39 Y. Lin, X. Han, J. Huang, H. Fu and C. Yu, *J. Colloid Interface Sci.*, 2009, **330**, 449–455.
40 J. L. Rose, B. V. Tata, V. K. Aswal, P. A. Hassan, Y. Talmon and L. Sreejith, *Eur. Phys. J. E: Soft Matter Biol. Phys.*, 2015, **38**, 4.
41 C. A. Dreiss, *Soft Matter*, 2007, **3**, 956–970.
42 K. Trickett and J. Eastoe, *Adv. Colloid Interface Sci.*, 2008, **144**, 66–74.
43 A. A. Serdyuk, A. B. Mirgorodskaya, I. V. Kapitanov, N. Gathergood, L. Y. Zakharova, O. G. Sinyashin and Y. Karpichev, *Colloids Surf., A*, 2016, **509**, 613–622.
44 R. Kumar, G. C. Kalur, L. Ziserman, D. Danino and S. R. Raghavan, *Langmuir*, 2007, **23**, 12849–12856.
45 S. R. Raghavan and E. W. Kaler, *Langmuir*, 2001, **17**, 300–306.
46 Y. Feng and Y. Han, *J. Mol. Liq.*, 2016, **218**, 508–514.
47 W. Kang, P. Wang, H. Fan, H. Yang, C. Dai, X. Yin, Y. Zhao and S. Guo, *Soft Matter*, 2017, **13**, 1182–1189.
48 J. N. Israelachvili, D. J. Mitchell and B. W. Ninham, *Biochim. Biophys. Acta, Biomembr.*, 1977, **470**, 185–201.
49 J. N. Israelachvili, D. J. Mitchell and B. W. Ninham, *J. Chem. Soc., Faraday Trans. 2*, 1976, **72**, 1525–1568.
50 T. Shikata, H. Hirata and T. Kotaka, *Langmuir*, 1988, **4**, 354–359.
51 S. J. Bachofer, U. Simonis and T. A. Nowicki, *J. Phys. Chem. B*, 1991, **95**, 480–488.
52 M. Vermathen, P. Stiles, S. J. Bachofer and U. Simonis, *Langmuir*, 2002, **18**, 1030–1042.